

Gas-induced perturbations on the gravitational wave in-spiral of live post-Newtonian LISA massive black hole binaries

MUDIT GARG ¹, ALESSIA FRANCHINI ¹, ALESSANDRO LUPI ², MATTEO BONETTI ^{3,4} AND LUCIO MAYER ¹

¹*Department of Astrophysics, University of Zurich, Winterthurerstrasse 190, CH-8057 Zürich, Switzerland*

²*DiSAT, Università degli Studi dell'Insubria, via Valleggio 11, I-22100 Como, Italy*

³*Dipartimento di Fisica "G. Occhialini", Università degli Studi di Milano-Bicocca, Piazza della Scienza 3, I-20126 Milano, Italy*

⁴*INFN, Sezione di Milano-Bicocca, Piazza della Scienza 3, I-20126 Milano, Italy*

ABSTRACT

We investigate the effect of dynamically coupling gas torques with gravitational wave (GW) emission during the orbital evolution of an equal-mass massive black hole binary (MBHB). We perform hydrodynamical simulations of eccentric MBHBs with total mass $M = 10^6 M_{\odot}$ embedded in a prograde locally isothermal circumbinary disk (CBD). We evolve the binary from 53 to 30 Schwarzschild radii separations using up to 2.5 post-Newtonian (PN) corrections to the binary dynamics, which allow us to follow the GW-driven in-spiral. For the first time, we report the measurement of gas torques onto a live binary a few years before the merger, with and without concurrent GW radiation. We also identify and measure a novel GW-gas coupling term in the in-spiral rate that makes gas effects an order of magnitude stronger than the gas-only contribution. We show that the evolution rate (\dot{a}) of the MBHB can be neatly expressed as the sum of the GW rate (\dot{a}_{GW}), the pure gas-driven rate (\dot{a}_{gas}), and their cross-term $\propto \dot{a}_{\text{GW}}\dot{a}_{\text{gas}}$. The source-frame gas-induced dephasing in the GW waveform is equivalent to losing ~ 0.5 GW cycles over the expected ~ 1700 cycles in a vacuum, which LISA should detect at redshift $z = 1$. We also propose a phenomenological model that captures the essence of simulations and can be used to perform Bayesian inference. Our results show how GWs alone can be used to probe the astrophysical properties of CBDs and have important implications on multi-messenger strategies aimed at studying the environments of MBHBs.

Keywords: accretion, accretion disks — black hole physics — gravitational waves — hydrodynamics — relativistic processes — (galaxies:) quasars: supermassive black holes

1. INTRODUCTION

The recent adoption of LISA (Amaro-Seoane et al. 2017; Colpi et al. 2024) and the development of TianQin (Li et al. 2024) and Taiji (Gong et al. 2021) will provide a powerful opportunity to detect gravitational waves (GWs) from coalescing near-equal mass massive black hole binaries (MBHBs) with masses $\sim 10^4$ - $10^7 M_{\odot}$. LISA can potentially detect MBHBs up to redshifts $z \lesssim 20$ and with high (e.g. $\lesssim 10^3$) signal-to-noise ratios (SNRs; Amaro-Seoane et al. 2017). MBHBs are a by-product of galaxy mergers (Begelman et al. 1980). When two galaxies merge, the massive black holes (MBHs)

hosted in their centre are expected to reach the centre of the remnant galaxy owing to the dynamical friction mechanism and form a bound binary at a pc scale. This binary can further proceed towards merger through the interaction with surrounding stars and gas until GWs are strong enough to take over and drive the binary to coalescence (Amaro-Seoane et al. 2023).

While interactions with stars in a tri-axial potential (e.g. Quinlan 1996; Preto et al. 2011; Khan et al. 2011) as well as a third close-by MBH (Blaes et al. 2002; Hoffman & Loeb 2007; Bonetti et al. 2019) can lead to a MBHB merger, they are relatively slow and rare mechanisms, respectively. In particular, sinking timescales of MBHBs due to three body encounters with stars can exceed a Gyr in the low density environments of stellar-disk dominated galaxies (Khan et al. 2018), the typical hosts of MBHs below $10^6 M_{\odot}$, that fall in the mass range

accessible by LISA. On the other hand, when the host galaxies are gas-rich, and have circumnuclear gas disks, then MBHBs can sink efficiently below pc separations (Mayer 2013; Souza Lima et al. 2020). At even smaller separations, below ~ 0.1 pc, the MBHB would carve a cavity, which results in the formation of a co-planar geometrically thin (Shakura & Sunyaev 1973) circumbinary disk (CBD; Escala et al. 2004; Cuadra et al. 2009; D’Orazio et al. 2016), allowing the binary to coalesce in less than 100 Myr (Haiman et al. 2009). Over the past few years, the interaction between a binary and its circumbinary disk has been studied extensively for various system parameters and thermodynamics assumptions using several different numerical hydrodynamical (HD) simulations (see e.g. Duffell et al. 2024). The general consensus is that circular nearly equal-mass binaries do undergo out-spiral in relatively thick CBDs while their in-spiral is aided by relatively thin (i.e. aspect ratio $H/R \lesssim 0.03$) CBDs (Tiede et al. 2020; Franchini et al. 2021, 2022).

Since MBHBs observable by LISA are likely to reside in gaseous environments (see, e.g. Mangiagli et al. 2022), it is important to study the effect of gas on the orbital evolution of the MBHB when it enters the LISA band. The first attempt in this direction was performed by several groups (Garg et al. 2022; Tiede et al. 2024; Zwick et al. 2024; Garg et al. 2024a) who measured the gas-induced dephasing in the LISA band by simply linearly adding the gas-driven evolution rate, computed in post-processing from 2D HD fixed binary orbit simulations, to the GW in-spiral rate. However, the scales considered in those numerical works are close to sub-pc, where GWs are still too weak to drive significant binary evolution. Furthermore, by adding the two contribution linearly, gas-induced dephasing studies might have ignored possible coupling between gas torques and GW-driven evolution, due to the lack of HD simulations where the two effects are naturally coupled together and the binary evolves under both processes at the same time.

Recently, Franchini et al. (2024) simulated an eccentric, live (Franchini et al. 2023), equal-mass $10^6 M_\odot$ MBHB embedded in a prograde $100M_\odot$ CBD by dynamically modeling the binary in-spiral with post-Newtonian (PN) corrections up to 2.5 order. They evolved the system for the final years of in-spiral, including the merger and post merger phase, to quantify possible electromagnetic (EM) counterparts. In this work, we use the same setup to simulate the same binary but now embedded in a lighter $5 M_\odot$ disk to properly investigate how gas perturbs the binary evolution rate. We then quantify for the first time the effect of gas-induced perturbations on waveforms using a live binary whose dynamics is com-

puted using PN corrections, thus including the interplay between energy and angular momentum change caused by both GW radiation and gas torques. With this simulation setup, the in-spiral is concurrently determined by GWs and gas, as opposed to co-adding the two effects in post-processing as previously done in the literature, allowing us to robustly quantify the gas-induced dephasing in the GW waveform and its detectability by LISA.

2. NUMERICAL SETUP

Following the approach used in Franchini et al. (2024), we model the binary using two equal-mass sink particles (Bate et al. 1995) that represent two Schwarzschild MBHBs with total mass $M = 10^6 M_\odot$, setting the respective sink radius to the innermost stable circular orbit (ISCO). We set the MBHB initial semi-major axis (SMA) to $a = 53.2$ Schwarzschild radii (r_s) and eccentricity to $e = 0.29$. Note that we start from the initial condition of the thin (i.e. aspect ratio $H/R = 0.03$) disk simulation in Franchini et al. (2024), which originated from a circular equal-mass binary evolved for 1000 binary orbits by Franchini et al. (2022). During the first 1000 orbits the eccentricity of the simulated live binary increases to $e = 0.29$ as a result of the interaction with the CBD. We here assume the disk to have a much smaller mass $M_d = 5M_\odot$.

We follow the evolution of the binary driven by both gas torques and PN corrections up to 2.5PN order using the code GIZMO (Hopkins 2015) until the binary reaches $= 30 r_s$ in separation in our GW+gas simulation, i.e. for ~ 1700 GW cycles. The implementation of the PN corrections to the binary dynamics follows the equations in Blanchet (2014). We include both conservative 1PN and 2PN terms, and radiative 2.5PN terms. The latter term generates the GW emission and leads to the decrease in binary SMA (\dot{a}_{GW}) and eccentricity only due to GWs. In order to integrate the 2.5PN equations, we implemented an intermediate predictor step to update the particle velocities at the end of the time step, accounting for the PN corrections, and re-enforcing the numerical stability of the integration algorithm. Our approach is similar to the one outlined in Sect. 6.2 of Liptai & Price (2019), except that we use a predictor-corrector approach instead of implementing the implicit kick-drift-kick one. In the initial setup the disk extended from $2a$ to $10a$. However during the first 1000 binary orbits, the cavity becomes eccentric and the inner edge increases to $\sim 3.5a$.

We also run two other simulations with the same setup. First, without the dissipative 2.5PN term to consider the binary evolution only due to the presence of the CBD. We run it for 1000 orbits to see any appre-

cial changes in the orbital quantities. This allows us to infer the SMA evolution rate only due to the gaseous disk (\dot{a}_{gas}) and therefore to disentangle its effect from the putative GW-gas cross term considered later. We then also run a simulation without the CBD in order to self-consistently obtain the evolution due to the PN terms only. This allows us to mitigate the numerical error in the integration when we compute the difference between the simulation with concurrent evolution under GWs and gas, and the one with PN terms only.

2.1. Post-processing analysis

The CBD typically affects the binary evolution by exerting both a gravitational torque (T_{grav}) and an accretion torque (T_{acc}). The first, just due to gravity, is essentially driven by any asymmetry in the gaseous flow while the latter is instead induced by the accretion of gas particles onto either MBHs. In particular, the accretion of gas alters not only the mass but also the angular momentum of the binary (see Franchini et al. 2021 for detailed calculations).

We can then express the overall gas effect in terms of a single simulation-calibrated parameter (Garg et al. 2022; Duffell et al. 2024)

$$\xi = \frac{T_{\text{grav}} + T_{\text{acc}}}{Ma^2\Omega}, \quad (1)$$

where $\dot{M} \equiv 0.02 f_{\text{Edd}}(M/10^6 M_{\odot})(M_{\odot}/\text{yr})$ is the accretion rate onto the binary for our assumed $\epsilon = 0.1$ radiative efficiency, $\Omega \equiv \sqrt{GM/a^3}$ is the binary orbital angular frequency, and $Ma^2\Omega$ is the viscous torque (Lin & Papaloizou 1986). ξ depends sensitively on the binary and disk parameters, in particular on the binary mass ratio q , disk shape and temperature, and may also depend upon the assumed equation of state. Previous sub-pc fixed binary orbit 2D Newtonian simulation predicted $|\xi| \sim 3$ (Dittmann & Ryan 2022) for $H/R \sim 0.03$.

We can therefore write down the SMA evolution rate due to gas torques for a quasi-circular binary as (Garg et al. 2024a)

$$\dot{a}_{\text{gas}} = 8\xi \frac{\dot{M}_z}{M_z} a = \xi f_{\text{Edd}} \frac{4}{25\text{Myr}} a, \quad (2)$$

where we infer both ξ and f_{Edd} from gas-only simulation to properly isolate any GW-gas coupling in the total SMA rate in the GW+gas simulation. Moreover, since the evolution only due to gas torques changes the SMA by a small quantity even after 1000 orbits, we extrapolate the results to smaller separations, i.e. until $30r_s$.

When the MBHB is dynamically evolving under both GWs and gas, there can be a coupled evolution that manifests in the form of a cross term \dot{a}_{GWgas} , whose

exact functional form is unknown. Therefore, the total SMA evolution rate can be written down as

$$\dot{a}_{\text{GW+gas}} = \dot{a}_{\text{GW}} + \dot{a}_{\text{gas}} + \dot{a}_{\text{GWgas}}, \quad (3)$$

where both \dot{a}_{gas} and \dot{a}_{GWgas} can be thought of as perturbative corrections to \dot{a}_{GW} in the final years of in-spiral.

Assuming the stationary phase approximation (Cutler & Flanagan 1994), where gas affects the phase but not the amplitude of the GW, we compute the dephasing in the time-domain GW waveform, caused by the presence of the CBD as

$$\delta\phi_{\text{gas}} = \Phi(\dot{a}_{\text{GW+gas}}) - \Phi(\dot{a}_{\text{GW}}), \quad (4)$$

where negative (positive) dephasing imply that gas speed-up (slow-down) the binary in-spiral. Here $\Phi(\dot{a})$ is the total accumulated GW phase for a given evolution rate \dot{a} between an initial (a_i) and a final (a_f) SMAs, and it can be expressed in radians as

$$\Phi(\dot{a}) = 2\pi \int_{a_i}^{a_f} da \frac{f}{\dot{a}}, \quad (5)$$

where $f \equiv \Omega/\pi$ is the GW frequency, that is twice the orbital frequency ($\Omega/2\pi$), under the assumption of quasi-circular binaries.

In the next section, we show the results together with the interpretation of our simulations.

3. RESULTS

We show disk morphologies and associated column densities at three SMAs – $a = 50r_s$, $a = 40r_s$, and $a = 30r_s$ – in Fig. 1 for the GW+gas simulation.¹ The gas morphology is similar, as expected, to the simulations presented in Franchini et al. (2024). We can clearly see the over-density at the cavity edge, i.e. the lump (Shi et al. 2012), precessing around the binary.

We measure the accretion rate in both our simulations and find a mean Eddington ratio of $f_{\text{Edd}} \approx 0.92$ for GW+gas simulation and $f_{\text{Edd}} \approx 1.20$ for the gas-only case. The slightly higher accretion rate in the gas-only case is a natural consequence of the fact that the binary does not start decoupling from the disk because of the lack of GW radiation, therefore the gas can flow inside the cavity and keep feeding the MBHB more effectively.

We then compute both gravitational and accretion torques directly from the simulations. We find that the magnitude of the accretion torque is $T_{\text{acc}} \sim 10^{-2} T_{\text{grav}}$. We show the evolution of the parameter ξ in Fig. 2

¹ disk morphology for gas-only simulation is similar to the left panel of Fig. 1.

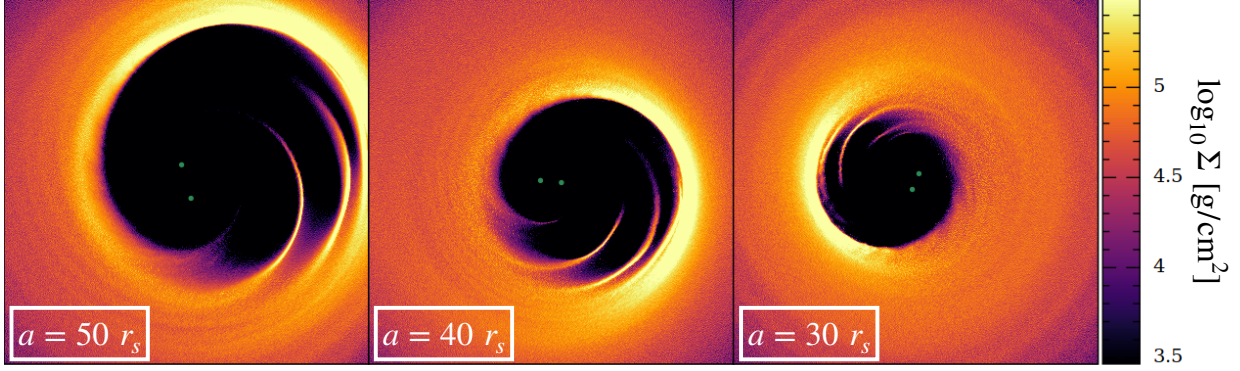


Figure 1. Column density (Σ) plots at three SMAs: $50r_s$ (left panel), $40r_s$ (middle panel), and $30r_s$ (right panel) for the binary evolution under both GW and gas. Here Σ varies between $\sim 10^{3.5}$ - 10^6 g/cm². While both the binary (green dots) and the cavity shrinks with time, cavity is becoming more eccentric also.

for GW+gas simulations as a function of SMA together with the average values of ξ for both GW+gas ($\bar{\xi}_{\text{GW+gas}} \approx -24$) and gas-only ($\bar{\xi}_{\text{gas}} \approx -36$) cases. Unsurprisingly, the mean gas effect is stronger when the binary is only evolving due to the gas torque. The parameter ξ is indeed decreasing in magnitude as the binary is in-spiraling further, since the gas effects are becoming weaker. Since the value of ξ does not change significantly with time in the gas-only simulation, the approximation we make in the parametrization of Eq. (1) is reasonable. It is worth noticing that for the computed gas-induced dephasing $\delta\phi_{\text{gas}}$ (see Section 3.1), most of the contribution is expected to originate from the early in-spiral phase, where the mean value of ξ is higher.

We also note that the high-frequency or sub-orbital fluctuations in Fig. 2 around the mean value may be measurable on their own, as suggested by analytical studies (Zwick et al. 2021, 2024). However, we focus on the secular trend in this work.

Once we subtract both \dot{a}_{GW} and \dot{a}_{gas} from the total SMA $\dot{a}_{\text{GW+gas}}$ rate inferred from the full GW+gas simulation, we find a non-negligible residual, which is the GW-gas coupling term introduced in Eq. (3). We propose to express this cross-term simply as

$$\dot{a}_{\text{GWgas}} \sim \zeta \dot{a}_{\text{GW}} \dot{a}_{\text{gas}}, \quad (6)$$

where ζ is also a simulation-calibrated parameter and we show its evolution in Fig. 3 as function of SMA. We find the average value of the cross-term to be $\approx -7.9 \times 10^{-5}$. The value of ζ is also decreasing as the binary is shrinking, similar to the evolution of ξ in Fig. 2. The almost constant evolution of ζ , marginally weakened by the in-spiral, may imply that our assumption to express $\dot{a}_{\text{GWgas}} \propto \dot{a}_{\text{GW}} \dot{a}_{\text{gas}}$ is not inaccurate.

3.1. Gas-induced dephasing and LISA observability

In this section, we compute the gas-induced dephasing $\delta\phi_{\text{gas}}$ in Eq. 4 in the source-frame between $= 53.2 r_s$

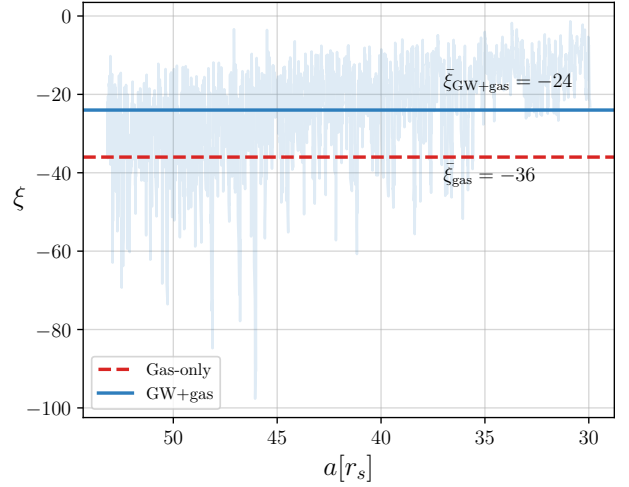


Figure 2. Gas torques onto the binary in terms of ξ as a function of the SMA for GW+gas simulation (light blue lines). We show average ξ values for GW+gas (solid blue line; $\bar{\xi}_{\text{GW+gas}} \approx -24$) and gas-only (dashed red line; $\bar{\xi}_{\text{gas}} \approx -36$) cases, respectively.

and $= 30 r_s$ with the initial eccentricity = 0.29 by using \dot{a}_{GW} inferred from the simulations and then considering the total SMA evolution rate $\dot{a}_{\text{GW+gas}}$ in three different ways.

- First of all directly from the GW+gas simulations, which leads to a dephasing $\delta\phi_{\text{gas}} = -3.21$ radians.
- The second estimate of the dephasing is performed by neglecting the GW-gas cross term, i.e. assuming $\dot{a}_{\text{GW+gas}} = \dot{a}_{\text{GW}} + \dot{a}_{\text{gas}}$, where \dot{a}_{gas} is computed from Eq. 2 with the gas-only simulation-calibrated parameters $\xi = -36$ and $f_{\text{Edd}} = 1.2$. This approach gives $\delta\phi_{\text{gas}} = -0.21$ radians.
- Lastly, we include the cross-term using the parametrization in Eq. 6 to have $\dot{a}_{\text{GW+gas}} = \dot{a}_{\text{GW}} +$

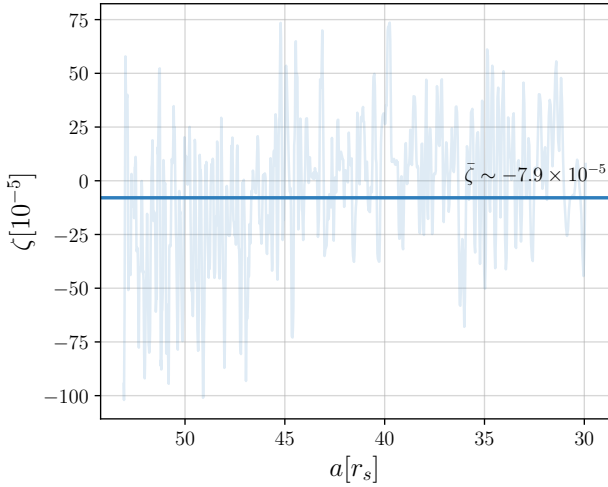


Figure 3. GW-gas coupling coefficient as a function of SMA (light blue lines) with its mean value $\bar{\zeta} = -7.9 \times 10^{-5}$ (solid blue line).

$\dot{a}_{\text{gas}} + \zeta \dot{a}_{\text{GW}} \dot{a}_{\text{gas}}$ with $\zeta = -7.9 \times 10^{-5}$. This results in $\delta\phi_{\text{gas}} = -3.63$ radians.

The dephasing we obtain neglecting the GW-gas cross term (i.e. assuming $\zeta = 0$) is an order of magnitude smaller than the value inferred with the non-zero cross term, so we caution that the GW-gas coupling might have a crucial role in the evolution of MBHBs in gaseous environments. Furthermore, the fact that the $\delta\phi_{\text{gas}}$ computed directly from the GW+gas simulation is almost the same as the dephasing computed by parametrizing the gas effect through the (simulation-calibrated) ξ and ζ parameters, provides a further consistency check of our model. The few percent difference between the two values might originate from the approximation made in assuming ξ and ζ to be constants with time.

We consider the evolution of our $10^6 M_{\odot}$ total mass eccentric MBHB at redshift $z = 1$ for one year of LISA observation. We therefore take an initial SMA of $a_i = 40r_s^{z=1}$ and an initial eccentricity $e = 0.2$, as the binary has partially circularized from its initial separation. We find the dephasing for $f_{\text{Edd}} = 1.2$, $\xi = -36$, and $\zeta = -7.9 \times 10^{-5}$ between $a_i = 40r_s^{z=1}$ and $a_f = 30r_s^{z=1}$ to be $\delta\phi_{\text{gas}} = -1.11$ radians, equivalent to losing ~ 0.2 GW cycles over the expected ~ 850 cycles from a vacuum eccentric binary evolving just under GWs. Since LISA should observe this event with $\text{SNR} \sim 1300$ (Garg et al. 2024d) and we typically need a given dephasing to be higher than $\sim 8/\text{SNR}$ (Derdzinski et al. 2021; Garg et al. 2022) to be detectable, we should be able to observe the computed $\delta\phi_{\text{gas}}$.

3.1.1. Analytical dephasing estimates

Since we would ultimately like to obtain a parametrized model for the GW+gas inspiral phase, we now use the orbital-averaged GW-driven inspiral rate at 2.5PN order from Peters (1964), i.e. $\dot{a}_{\text{GW}}^{\text{Peters}}$, for the GW only driven inspiral rate. Moreover, we also analytically construct the total SMA rate using the simulation-calibrated parameters ξ , f_{Edd} , and ζ to have

$$\dot{a}_{\text{GW+gas}}^{\text{analytical}} = \dot{a}_{\text{GW}}^{\text{Peters}} + \dot{a}_{\text{gas}} + \zeta \dot{a}_{\text{GW}}^{\text{Peters}} \dot{a}_{\text{gas}}. \quad (7)$$

If we repeat the dephasing computation done in § 3.1, then we get $\delta\phi_{\text{gas}} = -3.75$ radians. This is a few percent higher than the value calculated using only the simulations data. One possible reason is the inclusion of 1PN and 2PN terms in the simulations which, despite being conservative terms, lead to the precession of the MBHB eccentric orbit effectively altering its in-spiral rate. Another source of uncertainty in the dephasing estimate might reside in numerical errors. We have however compared our GW-only simulation with a numerical integration of the full (i.e. up to 2.5 order) PN evolution of the binary using an 8th order Runge-Kutta integrator finding negligible differences within the separations range we explored.

Even though we have only performed simulations for one set of binary-disk parameters, we can compute the expected dephasing for different values of the ξ and ζ parameters, which reflect the use of different system parameters in the simulations, through the analytical prescription in Eq. 7. In Fig. 4, we show $\delta\phi_{\text{gas}}$ for equal-mass circular MBHBs accreting at $f_{\text{Edd}} = 1$ for a one-year LISA observation until respective ISCO with varying $\xi \in [-1, -100]$, $\zeta \in [0, 2 \times 10^{-4}]$, $M \in \{10^5, 10^6\} M_{\odot}$, and $z \in \{1, 2\}$ to bracket reasonable parameters space. If we do not consider the GW-gas cross-term then the dephasing cannot be detectable by LISA for $M = 10^6 M_{\odot}$ MBHB at both redshifts for $|\xi| \lesssim 1$. The stronger dephasing with non-zero ζ again signifies the importance of considering the GW-gas cross-term in having observable gas effects on the GW waveform. Moreover, similar $\delta\phi_{\text{gas}}$ for different combinations of mass and redshift is possibly due to the cross-term dependence on $\dot{a}_{\text{GW}}^{\text{Peters}}$.

A perturbative correction to \dot{a}_{GW} with a functional form $\propto a^{n_g} \dot{a}_{\text{GW}}$ manifests at $-n_g$ PN relative order in the GW phase (Garg et al. 2024a). We have $n_g = 4$ and $n_g = 1$ for \dot{a}_{gas} and $\dot{a}_{\text{GW+gas}}$, respectively. Hence, an instantaneous frequency-depending dephasing enters the overall binary phase at relative -4 PN order due to evolution just under gas and at -1 PN relative order due to a GW-gas coupling.

Lastly, if we do not introduce a GW-gas coupling and try to explain the residual $(\dot{a}_{\text{GW+gas}} - \dot{a}_{\text{GW}})$ by using the model for \dot{a}_{gas} in Eq. 2, then the mean value of the

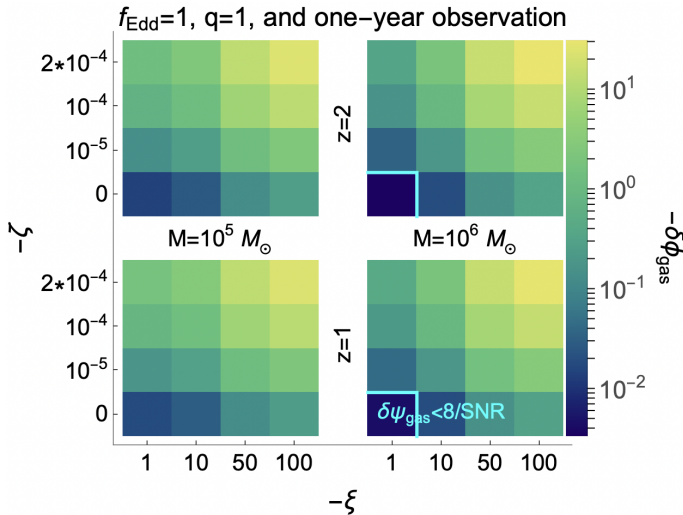


Figure 4. The gas-induced dephasing in the GW waveform, $\delta\phi_{\text{gas}}$ in radians, over a one-year LISA observation until ISCO as a function of the simulation-calibrated fudge factors ξ (represents gas torques) and ζ (represents GW-gas cross-term) for equal-mass MBHBs accreting at $f_{\text{Edd}} = 1$. In all four panels, we vary ξ from -1 to -100 and ζ from 0 to 2×10^{-4} . In the top two panels, we consider systems at redshift $z = 2$ and in the bottom two panels we assume $z = 1$. In the left two panels, we study a MBHB with source-frame total mass $M = 10^5 M_{\odot}$ and in the right panels we have $M = 10^6 M_{\odot}$. We also draw cyan lines to indicate the regions of non-observable dephasing by LISA, i.e. $\delta\phi_{\text{gas}} < 8/\text{SNR}$.

parameter ξ is ~ -360 . This implies that even a dephasing at -4PN relative order should be observable for our studied MBHB with or without concurrent eccentricity measurement (Garg et al. 2024a) in a realistic Bayesian data analysis setup, where all other binary parameters are also varying and a complete LISA response is considered. However, the GW-gas coupling is even more stronger than this, since it enters the GW phase at -1PN relative order, therefore causing a larger dephasing.

4. DISCUSSION AND CONCLUSION

We studied the interaction of an equal mass MBHB with its surrounding CBD during the late in-spiral stage, with and without concurrent GW emission, using 3D hydrodynamical simulations with a live binary. This approach provided us with the first direct measurement of how surrounding gas torques the binary when its in-spiral is already governed by GW emission, by means of the estimate of the ξ parameter in Eq. (1). We find that ξ is $\mathcal{O}(10)$ stronger than the previously explored scale-free/sub-pc regime. However, we caution that the comparison may not be fair as previous simulations carried out for the larger separation regime are predominantly 2D, assume a fixed binary orbit modelled under

Newtonian dynamics, and compute the effect of the energy and angular momentum loss by GW radiation in post-processing (Tang et al. 2018). In particular, Duffell et al. (2024) showed that 3D calculations give different magnitude torques compared to 2D and Franchini et al. (2023) argued that fixing the binary orbit leads again to a different gravitational torque. Moreover, we find that, consistently with our expectations, ξ is slightly weaker for GW+gas simulations ($\xi_{\text{GW+gas}} \sim -24$) with respect to gas-only study ($\xi_{\text{GW+gas}} \sim -36$), as shown in Fig. 2. This is expected since the binary is decoupling from the gas in the GW+gas simulation and therefore the effect of gas weakens with time.

Most importantly, we show that our results can be understood by introducing a novel coupling term between the energy loss by GWs and that due to gas in the orbital in-spiral rate, which we model through the product between the rate of change of the SMA due to GWs only and that due to gas only. The amplitude of this coupling term is pinpointed by a newly introduced simulation-calibrated parameter ζ , whose evolution is shown in Fig. 3 with an average value $\sim -7.9 \times 10^{-5}$. This implies richer gas features in the GW waveform than previously expected. While gas torques still induce a correction to the GW phase at the usual -4PN relative order (Garg et al. 2024a), our modeling of GW-gas cross-term enters the phase at -1PN relative order, leading to stronger phase shift by $\mathcal{O}(10)$ and higher likelihood of detection of gas perturbations with LISA. The -1PN relative order term may also allow us to break the degeneracy with concurrent eccentricity measurement using LISA (Garg et al. 2024a). Moreover, having a GW-gas coupling may change the expectation how the binary parameters in the LISA band are correlated with their values at sub-pc scales (Garg et al. 2024c). Lastly, ignoring gas effects while modeling MBHBs may lead to stronger apparent violations of general relativity than previously anticipated (Garg et al. 2024b) due to the new -1PN relative order term.

In this work, we studied one set of binary-disk parameters while in the future we plan on exploring the parameter space to understand how both ξ and ζ change. This exercise may also allow us to analytically model both simulation-calibrated parameters ξ and ζ . For instance, if the binary is embedded in a relatively thick disk ($H/R = 0.1$), we can expect to also have a significant contribution from mini-disks (i.e. disks around each binary component) that will introduce their own likely positive torque measurement (D’Orazio & Duffell 2021; Franchini et al. 2022; Siwek et al. 2023; Tiede & D’Orazio 2023) and probably a different sign for ζ .

Moreover, different numerical studies may also allow to check the robustness of our phenomenological model.

Lastly, we also find that, in the gas-only simulation, the eccentricity is linearly decreasing with the SMA. This needs to be further investigated in both sub-pc and near-merger regimes, and we plan to do so in the future.

It is to be noted that we employ PN corrections as an approximation since we do not run general relativistic magnetohydrodynamical (GRMHD) simulations. Current GRMHD simulations only study the binary evolution just a few days before merger (Gutiérrez et al. 2022; Avara et al. 2023) to integrate only a few orbits because of the prohibitive computational cost. Therefore, since the majority of the gas-driven effects on the binary inspiral occurs at separations $a \gtrsim 30 r_s$, our approach is currently the best available method to investigate the orbital dephasing due to the presence of the gas and where PN corrections are may be adequate.

A possible caveat in our work is that our binary is moderately eccentric (~ 0.3) just a few years before the merger, which will require the eccentricity to be extremely high when GWs take over at milli-pc scales. However, since $e \sim 0.3$ arises naturally from our initial condition requiring a steady-state disk before setting the

physical scale of $a \sim 53r_s$, the only truly realistic way to initialize the system is to evolve the binary starting from a much wider separation. This, however, would increase the computational cost dramatically. We plan to investigate alternative procedures in the setup of the simulations in order to reduce the computational cost and mitigate this issue in the future.

In summary, our results can facilitate the modeling of gas effects perturbing GW waveforms, which in turn will allow to better quantify how effectively LISA can place constraints on the environment of MBHBs, eventually opening the pathway for more informed synergies between GWs and EM observations. Furthermore, our work, being the first of its kind with PN dynamics and a live binary in 3D, while still assuming a simple isothermal equation of state, provides a starting point for future hydrodynamical studies with additional physics, including, for example, more realistic thermodynamics.

ACKNOWLEDGEMENTS

MG acknowledge support from the Swiss National Science Foundation (SNSF) under the grant 200020_192092. The authors also acknowledge use of the NumPy (Harris et al. 2020) and Matplotlib (Hunter 2007).

REFERENCES

- Amaro-Seoane, P., Audley, H., Babak, S., et al. 2017, arXiv e-prints, arXiv:1702.00786.
<https://arxiv.org/abs/1702.00786>
- Amaro-Seoane, P., Andrews, J., Arca Sedda, M., et al. 2023, *Living Reviews in Relativity*, 26, 2, doi: 10.1007/s41114-022-00041-y
- Avara, M. J., Krolik, J. H., Campanelli, M., et al. 2023, arXiv e-prints, arXiv:2305.18538, doi: 10.48550/arXiv.2305.18538
- Bate, M. R., Bonnell, I. A., & Price, N. M. 1995, *MNRAS*, 277, 362, doi: 10.1093/mnras/277.2.362
- Begelman, M. C., Blandford, R. D., & Rees, M. J. 1980, *Nature*, 287, 307, doi: 10.1038/287307a0
- Blaes, O., Lee, M. H., & Socrates, A. 2002, *ApJ*, 578, 775, doi: 10.1086/342655
- Blanchet, L. 2014, *Living Reviews in Relativity*, 17, 2, doi: 10.12942/lrr-2014-2
- Bonetti, M., Sesana, A., Haardt, F., Barausse, E., & Colpi, M. 2019, *MNRAS*, 486, 4044, doi: 10.1093/mnras/stz903
- Colpi, M., Danzmann, K., Hewitson, M., et al. 2024, arXiv e-prints, arXiv:2402.07571, doi: 10.48550/arXiv.2402.07571
- Cuadra, J., Armitage, P. J., Alexander, R. D., & Begelman, M. C. 2009, *MNRAS*, 393, 1423, doi: 10.1111/j.1365-2966.2008.14147.x
- Cutler, C., & Flanagan, É. E. 1994, *PhRvD*, 49, 2658, doi: 10.1103/PhysRevD.49.2658
- Derdzinski, A., D’Orazio, D., Duffell, P., Haiman, Z., & MacFadyen, A. 2021, *MNRAS*, 501, 3540, doi: 10.1093/mnras/staa3976
- Dittmann, A. J., & Ryan, G. 2022, *MNRAS*, 513, 6158, doi: 10.1093/mnras/stac935
- D’Orazio, D. J., & Duffell, P. C. 2021, *ApJL*, 914, L21, doi: 10.3847/2041-8213/ac0621
- D’Orazio, D. J., Haiman, Z., Duffell, P., MacFadyen, A. I., & Farris, B. D. 2016, *Mon. Not. Roy. Astron. Soc.*, 459, 2379, doi: 10.1093/mnras/stw792
- Duffell, P. C., Dittmann, A. J., D’Orazio, D. J., et al. 2024, *ApJ*, 970, 156, doi: 10.3847/1538-4357/ad5a7e
- Escala, A., Larson, R. B., Coppi, P. S., & Mardones, D. 2004, *ApJ*, 607, 765, doi: 10.1086/386278
- Franchini, A., Bonetti, M., Lupi, A., & Sesana, A. 2024, *A&A*, 686, A288, doi: 10.1051/0004-6361/202449206
- Franchini, A., Lupi, A., & Sesana, A. 2022, *ApJL*, 929, L13, doi: 10.3847/2041-8213/ac63a2

- Franchini, A., Lupi, A., Sesana, A., & Haiman, Z. 2023, MNRAS, 522, 1569, doi: [10.1093/mnras/stad1070](https://doi.org/10.1093/mnras/stad1070)
- Franchini, A., Sesana, A., & Dotti, M. 2021, MNRAS, 507, 1458, doi: [10.1093/mnras/stab2234](https://doi.org/10.1093/mnras/stab2234)
- Garg, M., Derdzinski, A., Tiwari, S., Gair, J., & Mayer, L. 2024a, arXiv e-prints, arXiv:2402.14058, doi: [10.48550/arXiv.2402.14058](https://doi.org/10.48550/arXiv.2402.14058)
- Garg, M., Derdzinski, A., Zwick, L., Capelo, P. R., & Mayer, L. 2022, MNRAS, 517, 1339, doi: [10.1093/mnras/stac2711](https://doi.org/10.1093/mnras/stac2711)
- Garg, M., Sberna, L., Speri, L., Duque, F., & Gair, J. 2024b, arXiv e-prints, arXiv:2410.02910, <https://arxiv.org/abs/2410.02910>
- Garg, M., Tiede, C., & D’Orazio, D. J. 2024c, arXiv e-prints, arXiv:2405.04411, doi: [10.48550/arXiv.2405.04411](https://doi.org/10.48550/arXiv.2405.04411)
- Garg, M., Tiwari, S., Derdzinski, A., et al. 2024d, MNRAS, 528, 4176, doi: [10.1093/mnras/stad3477](https://doi.org/10.1093/mnras/stad3477)
- Gong, X., Xu, S., Gui, S., Huang, S., & Lau, Y.-K. 2021, in Handbook of Gravitational Wave Astronomy (Springer Singapore), 24, doi: [10.1007/978-981-15-4702-7_24-1](https://doi.org/10.1007/978-981-15-4702-7_24-1)
- Gutiérrez, E. M., Combi, L., Noble, S. C., et al. 2022, ApJ, 928, 137, doi: [10.3847/1538-4357/ac56de](https://doi.org/10.3847/1538-4357/ac56de)
- Haiman, Z., Kocsis, B., & Menou, K. 2009, ApJ, 700, 1952, doi: [10.1088/0004-637X/700/2/1952](https://doi.org/10.1088/0004-637X/700/2/1952)
- Harris, C. R., Millman, K. J., van der Walt, S. J., et al. 2020, Nature, 585, 357, doi: [10.1038/s41586-020-2649-2](https://doi.org/10.1038/s41586-020-2649-2)
- Hoffman, L., & Loeb, A. 2007, MNRAS, 377, 957, doi: [10.1111/j.1365-2966.2007.11694.x](https://doi.org/10.1111/j.1365-2966.2007.11694.x)
- Hopkins, P. F. 2015, MNRAS, 450, 53, doi: [10.1093/mnras/stv195](https://doi.org/10.1093/mnras/stv195)
- Hunter, J. D. 2007, Computing in Science & Engineering, 9, 90, doi: [10.1109/MCSE.2007.55](https://doi.org/10.1109/MCSE.2007.55)
- Khan, F. M., Capelo, P. R., Mayer, L., & Berczik, P. 2018, ApJ, 868, 97, doi: [10.3847/1538-4357/aae77b](https://doi.org/10.3847/1538-4357/aae77b)
- Khan, F. M., Just, A., & Merritt, D. 2011, ApJ, 732, 89, doi: [10.1088/0004-637X/732/2/89](https://doi.org/10.1088/0004-637X/732/2/89)
- Li, E.-K., Liu, S., Torres-Orjuela, A., et al. 2024, arXiv e-prints, arXiv:2409.19665, <https://arxiv.org/abs/2409.19665>
- Lin, D. N. C., & Papaloizou, J. 1986, ApJ, 309, 846, doi: [10.1086/164653](https://doi.org/10.1086/164653)
- Liptai, D., & Price, D. J. 2019, MNRAS, 485, 819, doi: [10.1093/mnras/stz111](https://doi.org/10.1093/mnras/stz111)
- Mangiagli, A., Caprini, C., Volonteri, M., et al. 2022, Phys. Rev. D, 106, 103017, doi: [10.1103/PhysRevD.106.103017](https://doi.org/10.1103/PhysRevD.106.103017)
- Mayer, L. 2013, Classical and Quantum Gravity, 30, 244008, doi: [10.1088/0264-9381/30/24/244008](https://doi.org/10.1088/0264-9381/30/24/244008)
- Peters, P. C. 1964, PhD thesis, California Institute of Technology
- Preto, M., Berentzen, I., Berczik, P., & Spurzem, R. 2011, ApJL, 732, L26, doi: [10.1088/2041-8205/732/2/L26](https://doi.org/10.1088/2041-8205/732/2/L26)
- Quinlan, G. D. 1996, NewA, 1, 35, doi: [10.1016/S1384-1076\(96\)00003-6](https://doi.org/10.1016/S1384-1076(96)00003-6)
- Shakura, N. I., & Sunyaev, R. A. 1973, A&A, 500, 33
- Shi, J.-M., Krolik, J. H., Lubow, S. H., & Hawley, J. F. 2012, ApJ, 749, 118, doi: [10.1088/0004-637X/749/2/118](https://doi.org/10.1088/0004-637X/749/2/118)
- Siwek, M., Weinberger, R., & Hernquist, L. 2023, MNRAS, 522, 2707, doi: [10.1093/mnras/stad1131](https://doi.org/10.1093/mnras/stad1131)
- Souza Lima, R., Mayer, L., Capelo, P. R., Bortolas, E., & Quinn, T. R. 2020, ApJ, 899, 126, doi: [10.3847/1538-4357/aba624](https://doi.org/10.3847/1538-4357/aba624)
- Tang, Y., Haiman, Z., & MacFadyen, A. 2018, MNRAS, 476, 2249, doi: [10.1093/mnras/sty423](https://doi.org/10.1093/mnras/sty423)
- Tiede, C., & D’Orazio, D. J. 2023, arXiv e-prints, arXiv:2307.03775, <https://arxiv.org/abs/2307.03775>
- Tiede, C., D’Orazio, D. J., Zwick, L., & Duffell, P. C. 2024, ApJ, 964, 46, doi: [10.3847/1538-4357/ad2613](https://doi.org/10.3847/1538-4357/ad2613)
- Tiede, C., Zrake, J., MacFadyen, A., & Haiman, Z. 2020, ApJ, 900, 43, doi: [10.3847/1538-4357/aba432](https://doi.org/10.3847/1538-4357/aba432)
- Zwick, L., Capelo, P. R., Bortolas, E., et al. 2021, MNRAS, 506, 1007, doi: [10.1093/mnras/stab1818](https://doi.org/10.1093/mnras/stab1818)
- Zwick, L., Tiede, C., Trani, A. A., et al. 2024, arXiv e-prints, arXiv:2405.05698, doi: [10.48550/arXiv.2405.05698](https://doi.org/10.48550/arXiv.2405.05698)